Ionization, Energetics, and Geometry of the Phenol−S Complexes (S = H_2O, CH_3OH, and CH_3OCH_3)

Alexa Courty, Michel Mons,* Iliana Dimicoli, François Piuzzi, Valérie Brenner, and Philippe Millié

Service des Photons, Atomes et Molécules, Commissariat à l'Energie Atomique, Centre d'Etudes de Saclay, Bât. 522, 91191 Gif-sur-Yvette Cedex, France

Received: January 28, 1998; In Final Form: April 6, 1998

The present study combines both experiment and molecular modeling to describe the photoionization behavior of the gas-phase hydrogen-bonded complexes of phenol with water, methanol, and dimethyl ether, in particular the occurrence of fragmentation following ionization. Using the two-color two-photon resonant ionization laser technique, the threshold for dissociative ionization of these species has been measured. For the first time, precise binding energies have been deduced for the neutral species: D_0(phenol−H_2O) = 243 ± 5 meV and D_0(phenol−CH_3OH) = 265 ± 8 meV. Using a semiempirical potential model, the minimum energy structures of both neutral and ionic species have been determined. This theoretical study has emphasized the role of the dispersive interactions in the geometry of these neutral complexes, in particular the interactions between the alkyl group of the solvent molecule (CH_3 in the case of methanol or dimethyl ether) and the π-cloud of the aromatic molecule. In addition, the comparison between the neutral and ionic geometry of these complexes has allowed us to account qualitatively for the changes in the ionization properties within the complex series, namely in their zero kinetic-energy photoelectron spectra.

1. Introduction

The hydrogen-bonded 1:1 complexes between an organic proton donor and an acceptor molecule have been extensively studied since some decades in the liquid phase.[1] For example, complexes of phenol with several proton acceptors were investigated. In particular, temperature-dependent infrared absorption measurements allowed the experimentalists to compare the strength of the hydrogen bond, as measured by the binding enthalpy of the condensed phase complex, to the spectroscopic red shift of the OH bond frequency of the phenol molecule.[1] A nearly linear correlation was found between these two measurements for a series of bases spread over a wide range on the basicity scale. Such an observation clearly justifies the use of the spectral shift of the OH vibration of phenol as a spectroscopic indicator of the strength of the hydrogen bond. These spectroscopic techniques, however, do not provide any data for complexes of phenol with bases also containing OH vibrators, in particular water, because of the overlap of the several OH infrared bands.

In the past decade, gas phase 1:1 complexes have been extensively studied[2] as the first step of proton transfer in clusters, in particular, complexes of phenol[3−29] or 1-naphthol[30,31] with several solvents. Several experimental techniques were used to characterize these systems: laser-induced fluorescence and resonant two-photon ionization for the electronic spectroscopy,[3−9,11,18,25] zero kinetic energy (ZEKE) photoelectron spectroscopy,[14−16,22,26,28] and more recently, infrared[13,20,23,29] or Raman[12] spectroscopy combined with a mass-selective ionization detection, as well as microwave spectroscopy.[19] The low temperature of these jet-formed species leads to very narrow infrared absorption bands, so that the OH vibrators of the phenol molecule and its solvent can be easily distinguished. The perturbed OH vibration is now available for some complexes, in particular the 1:1 complexes of phenol with water,[13] ammonia, and substituted aromatic amines.[29]

Concerning the energetics of the gas-phase neutral complexes, however, very little experimental data exist in the literature. Only very recently, the binding energy D_0 of the 1:1 complexes of a bicyclic aromatic analogue of phenol (1-naphthol) with several bases (water, methanol, ammonia) has been investigated in the group of Leutwyler,[31] using a technique developed by these authors, which combines stimulated emission pumping and resonant two-photon ionization detection. For the complexes of phenol, apart from a short experimental study of phenol−ammonia by Mikami and co-workers,[23] the ab initio calculations, carried out at several levels of theory, are our only guidelines to the energetics of the phenol−water complex and its analogues.[11,12,17,21,27,31]

For this reason, we have developed a dual approach to the problem of the energetics of the phenol complexes.

We have undertaken a direct measurement of the binding energies of the phenol complexes in order to provide a consistent corpus of experimental data, which can be used as benchmarks for the validation of model potentials or of ab initio calculations.

On the other hand, we have modeled the phenol complexes using a semiempirical model recently applied sucessfully to similar hydrogen-bound complexes.[32] This kind of model offers an alternative approach to ab initio calculations, in particular the possibility of performing an extensive exploration of the potential energy surface of the species, as well as to carry out molecular dynamics studies of the 1:1 and even 1:*n* complexes. In addition, whereas the 1:1 complex of phenol with water has been extensively investigated using several ab initio methods,[11,12,17,21,27,31] calculations on other complexes of phenol are rather sparse.[24,25] Moreover, these calculations do not take into account dispersive interactions in the geometry optimization, which can be troublesome for species in which this type of

S1089-5639(98)00918-9 CCC: $15.00
Published on Web 05/29/1998

interaction is expected to be significant, for example, when the solvent molecule possesses an alkyl moiety.[32] Moreover, the semiempirical model used in the present work also enables the treatment of the ionic systems, thus permitting the comparison of both neutral and ionic geometries. Such data can be used to qualitatively understand the ionization properties of these species, in particular their ZEKE photoelectron spectra. This appears even more interesting since a series of experimental ZEKE spectra of the complexes of phenol with water, methanol and dimethyl ether carried out by Müller-Dethlefs and co-workers[14−16,22,26,28] could not be satisfactorily interpreted on the basis of ab initio calculations alone.[16] In particular, the geometry change between neutral and ionic complexes was not found to differ sufficiently to account for the progressions observed on several intermolecular vibrational ionic modes, measured in the ZEKE spectra of phenol−methanol and phenol−DME.[16,26,28]

In the present paper, we report a precise measurement of the binding energy D_0 of the 1:1 complexes of phenol with a series of O-containing proton acceptors: water, methanol, and dimethyl ether (DME). The technique used, inspired from the ionization properties of these species, consists in detecting the appearance threshold of the phenol ion in a two-color two-photon ionization experiment. Besides the experiment itself, we have used the semiempirical model developed in our group to investigate energetics, equilibrium structures, and ionization properties of these species.

2. Experimental Setup

The experimental setup, already described elsewhere,[33] combines a supersonic beam, dye lasers, and a reflectron-type TOF mass spectrometer. The neutral complexes of phenol with water or methanol are formed by the expansion of a gas mixture containing the room temperature vapor pressure of phenol and water or methanol in helium. The complex of phenol with dimethyl ether (DME) was formed using a gaseous mixing of 10% of DME in He as carrier gas. The pulsed expansion is generated by a commercial pulsed valve (General Valve) of 0.4 mm diameter nozzle operating at a frequency of 10 Hz. The jet is skimmed before entering the mass spectrometer (MS) chamber (pressure less than 10^{-6} Torr during operation) parallel to the spectrometer axis. The complexes are excited in the S_1 state by the beam of two dye lasers (Lambda Physik FL 2002) pumped by an excimer laser (Lambda Physik EMG 201) and then ionized by the frequency-doubled beam of a visible (640−470 nm) optical parametric oscillator (YAG-pumped VEGA, 7 ns pulse length, 0.2 cm^{-1} spectral width, BMI). The two pulsed beams were electronically synchronized in order to cross simultaneously the pulsed molecular beam in the interaction chamber of the mass spectrometer. The ions thus formed are extracted, accelerated in the spectrometer source, and deflected from the jet axis in order to separate them from the neutral beam as well as to send them to the electrostatic mirror entrance. After reflection and drift in a second field-free region, ions are detected in a microchannel plate device. The mass spectra are averaged on a numeric oscilloscope (LeCroy 9350) and then processed with a LabView-based computer program. The fragmentation rate was carefully measured by integrating the parent and daughter ion signals and subtracting the signal baseline. Although the mass spectrometer is operating in the reflectron mode, the mass loss corresponding to the phenol-water fragmentation is nevertheless too large to allow the reflectron to detect, at their true mass, the daughter ions due to metastable decay in the field-free region. Consequently, the effective time window for fragmentation in the experiment corresponds to ion lifetimes of less than 1 μs. The corresponding kinetic shift is nevertheless expected to remain small, due to the small number of intermolecular degrees of freedom of the complexes.

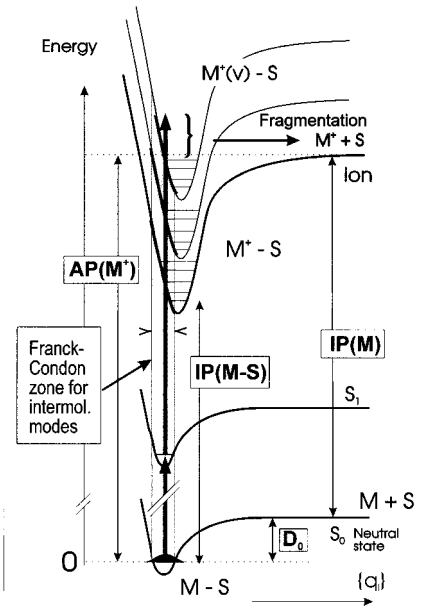

Figure 1. Principle of the measurement of binding energies by dissociative resonant two-photon ionization.

3. Experimental Results

3.1. Principle of the Experiment. The experiment is based on the possibility of exciting the complex ion in very excited inter- or intramolecular vibrational levels, located in the region of its dissociation threshold (Figure 1). Such vibrational excitations in the ion will be encountered (i) if one can efficiently excite intramolecular vibrational level of the aromatic molecule, in which case the vibrational redistribution will transfer the vibrational energy in the intermolecular modes, and/or (ii) if one can directly excite the intermolecular modes. Both excitations are governed by the Franck−Condon factors between the electronic state that undergoes ionization (S_0 in a one-photon ionization, S_1 in a two-photon ionization) and the ground state ion. Concerning the intramolecular vibrations, R2PI-PES studies show that several vibrational states are accessible in the phenol ion, up to the energetic limit.[34] Concerning the intermolecular modes, the pioneering work of Ito et al. on the photoionization of these studies already suggested that the ionization process was not adiabatic for the H-bonded clusters of this type.[5] This has been brightly confirmed by the photoionization spectra[7] of phenol−water and the ZEKE spectra of Müller-Dethlefs and co-workers[14−16,22,26,28] on the complexes of phenol with water, methanol, ethanol, and DME. They all exhibit at least a long progression in the intermolecular stretching mode, assigned to a shrinkage of the H-bond upon ionization, accompanied in some cases (with methanol and DME) by progressions in other intermolecular modes. The same ZEKE spectra also confirm the excitation of intramolecular modes in combination with intermolecular modes and exhibit an intensity envelope, which is still increasing up to internal energies of 2000 cm^{-1} in the ion. This point strongly suggests that we should be able to vibrationally excite these complexes of phenol, sufficiently high in energy, to observe their fragmentation.

3.2. One-Color Mass Spectra. The most pertinent test to establish the feasibility of the binding energy measurement consists in the measurement of the fragmentation rate in a one-

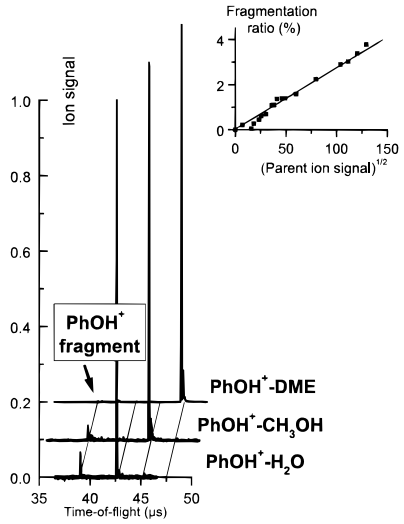

Figure 2. Comparison of the time-of-flight spectra obtained after one-color resonant two-photon ionization of the 1:1 complexes of phenol with water, methanol, and dimethyl ether. The laser was tuned to the origin $S_1 \leftarrow S_0$ transition of these species, as given in ref 16. In the insert is also shown the fragmentation ratio measured as a function of the square root of the parent intensity, which should be roughly proportional to the pulse intensity. The linear dependence suggests that the probability of ion excitation can significantly influence fragmentation ratios measured. In the time-of-flight spectra presented, as well as in the present experiment, the laser intensity was kept small enough to have negligible ion excitation (less than 2%).

color two-photon resonant ionization experiment. Indeed, in these systems, the one-color resonant ionization via the S_1 state leads to a wide range of possible energy content (~1 eV) in the ion (Figure 1). One should thus be able to form all the vibrational ionic levels accessible in the ion according to Franck−Condon principle. In that case, the observation of a nonvanishing fragmentation rate would indicate that fragmentation is possible; in other terms, the Franck−Condon envelope extends beyond the dissociation limit of the ion (Figure 1).

The mass spectra obtained by pumping the origin band of the $S_1 \leftarrow S_0$ transition[16] of the 1:1 complex of phenol with water, methanol, and DME are given in Figure 2. In each spectrum, the complex peak is the most prominent and no peak of higher mass is present in the spectrum, which illustrates the high selectivity of the $S_1 \leftarrow S_0$ excitation. At smaller masses, a weak phenol$^+$ peak is observed for phenol−water and phenol−methanol. No corresponding signal is detected with DME within the noise limit. It should be noted that these spectra have been carried out at very low laser fluences ($F < 500$ kW/cm^2). This condition must be fulfilled in order to prevent the absorption of an additional photon in the ion due to the presence of excited electronic ionic states in the energy region of the third photon. Absorption of a photon by the ion is indeed a rather efficient process that has been recently proved as a cause for major misassignments, because of the subsequent very fast fragmentation after ionic excitation.[35] The insert of Figure 2 illustrates the linear dependence expected for the fragmentation ratio τ (defined as the fragment intensity over the total parent + fragment ion intensity) with the square root of the parent intensity I_P, which is expected to vary with the laser fluence, providing that both the probability of excitation in the ion and the fragmentation ratio remain small. Such a dependence has allowed us to determine the laser intensity threshold below which the effects of ion excitation can be neglected for each complex.

From these one-color mass spectra, it turns out that, from water to DME, the fragmentation ratio varies as follows: 9% with water, 5% with methanol, and vanishes for DME. Since it seems reasonable to assume that (i) the Franck−Condon factors are similar in these species for the intramolecular modes and (ii) the Franck−Condon envelope should not be too different for the intermolecular modes, as is suggested by the ZEKE spectra of these complexes, in the region of the ionization energy,[14−16,22,26,28] one can postulate that the energetically accessible region has the same extent in the complex ion from the ion well bottom. In this case, the decrease observed in the fragmentation probability from water to DME should be ascribed to the increasing binding energy of the complex ion. This is in agreement with the trend in the ionization potential shift (δIP) measured by Müller-Dethlefs and co-workers when going from water to DME complex (−4601, −5421, and −6024 cm^{-1} respectively, expressed relative to the IP of phenol[15,16]), assuming that the trend in the δIP's is mainly controlled by the ion binding energies.

These results also show that a two-color experiment, in which the appearance threshold of the phenol$^+$ ion is detected, is feasible in the case of the phenol−water and phenol−methanol complexes.

3.3. Two-Color Fragmentation Spectra. The appearance threshold of the phenol$^+$ fragment ion has been measured in a two-color resonant two-photon ionization experiment on the phenol−water and the phenol−methanol complexes. The peak intensity of both the parent and daughter ions were integrated over the peak time width. Great care was taken to limit as far as possible the laser intensities in order to prevent absorption of $h\nu_1$ or $h\nu_2$ photons in the ion. The one-color residual signal due to the first laser alone, which typically represented 10% of the signal, was systematically subtracted. The signal due to the second laser alone was found to be negligible in the spectral region of interest.

The insert in Figure 2 shows the fragmentation probability as a function of the total $h\nu_1 + h\nu_2$ photon energy. For both complexes studied, the fragmentation ratio is found to increase nearly linearly from a well-defined onset. The appearance energy was taken at the intersect of the linear slope with the below threshold background, which is assigned to the undesired three-photon processes evoked above. The ionization energy of phenol, measured within the same experimental conditions, in particular within the same extraction electric field, allows us to yield a value of the ground-state binding energy of the complex. Our best values (243 ± 5 meV for phenol−water and 265 ± 8 meV for phenol−methanol) were obtained from an average over five different fragmentation spectra (Figure 3). The uncertainties mentioned account for the reproducibility of the experiment.

One can observe that the values derived from this procedure should be a priori considered as upper values of the binding energy, for two reasons:

(i) For the dissociation to occur, it is necessary to populate vibrational levels of the ion. The precision upon the appearance threshold will thus depend on the density of vibrational levels accessible in the corresponding energy region. In the case of the water complex for instance, the density of accessible levels can be rather sparse, as suggested by the low band density observed in the ZEKE spectrum, which is mainly due to a progression in the intermolecular stretching mode. In order to compensate for this bias, we have taken the appearance threshold as the intersect of the linear increase of τ with the background.

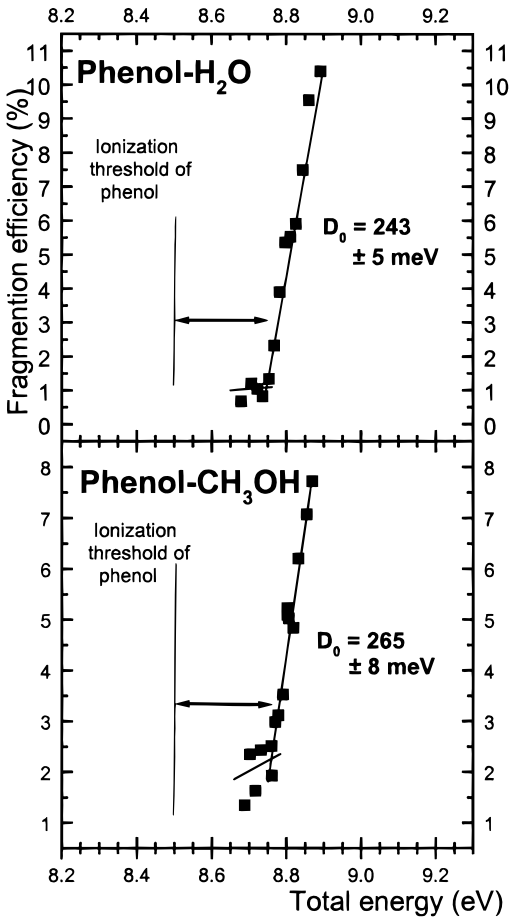

Figure 3. Fragmentation efficiencies obtained after two-color ionization of the 1:1 complexes of phenol with water and methanol as a function of total photon energy $\nu_1 + \nu_2$. For reference, the two-color photoionization spectrum of the phenol molecule is also given.

(ii) Fragmentation is detected in a time-of-flight mass spectrometer, whose time window does not exceed one microsecond; in other terms, one is not able to distinguish between parent and daughter ions after 1 μs: this is classically the reason for the existence of a kinetic shift. However, in the systems presently studied, which have only 6 pertinent degrees of freedom, the kinetic shift is thought to be negligible.[36] This has been checked by comparing the binding energy of the benzene dimer measured in the present experiment (73 ± 5 meV) with the value given by Neusser and co-workers (70 ± 10 meV), who detected the metastable fragmentation up to 30 μs after ionization.[36]

4. Theoretical Methodology

For van der Waals complexes, the determination of the equilibrium structures and their binding energy requires a rather correct evaluation of all contributions (electrostatic, polarization, repulsion, and dispersion) to the interaction energy and of their dependence upon the intermolecular coordinates since these interactions exhibit different behaviors. In the classical quantum chemistry approach, extended basis sets and highly correlated ab initio methods have to be used: at least, a geometry optimization at the second-order Møller−Plesset perturbation theory (MP2) within double-ζ plus polarization basis set in order to account for the correlation effects, namely, the dispersion forces as well as a correct value of the permanent electric moments of each molecular subunit. Such calculations are, however, too time-consuming to be directly applied to large systems, and in any case, intractable for exhaustive exploration of potential energy surfaces. Moreover, another well-known difficulty of this approach is the so-called basis set superposition error (BSSE) which arises from the use of finite atomic basis sets and which reach the same order of magnitude as the interaction energy. Even if this error may be estimated when computing the interaction energy, its dependence upon the intermolecular coordinates cannot be easily evaluated and in our knowledge, no automatic geometry optimization can be performed, taking into account this effect. We have therefore decided to perform our theoretical study with a completely different strategy and to use a semiempirical model for intermolecular interactions.

4.1. Intermolecular Interactions. We have used the semiempirical method initially developed by Claverie et al.,[37−39] based on the exchange perturbation theory. This method has already been successfully applied to van der Waals complexes.[32,40,41] The details of the method have already been described.[37−39,42,43] At the second order of this treatment, the interaction energy is obtained as a sum of four terms: electrostatic, polarization, dispersion, and short-range repulsion. Each contribution is expressed by simplified analytical formulas which give a reliable description of interactions for all intermolecular distances:

(i) The electrostatic term is calculated as the sum of multipole−multipole interactions. From the exact multipolar multicentric development of the electronic distribution (derived from ab initio correlated wave function of each molecular subunit), a simplified representation is generated using a systematic procedure of reduction of the number of centers.[44] We thus determine a set of multipoles (a monopole, a dipole, and a quadrupole on each atom and one point per chemical bond) for each molecular subunit.

(ii) The polarization energy is the sum of the polarization energies of each molecular subunit due to the electric field created by the multipoles of all the other molecular subunits. The polarizability of centers is evaluated from mean bond experimental dipolar polarizabilities according to the number of electrons of atoms involved in the bonds and lone pairs. In this way, the most important *n*-body terms are taken into account but contributions of high order as polarization via quadrupole polarizability, hyperpolarization, or back polarization (polarization by the induced moments) are neglected. This assumption is justified for neutral systems since the polarization energy represents only 5−10% of the total interaction energy. For charged systems, this approach is no longer adopted because of the much more important polarization contribution to the interaction energy. For these reasons, ab initio calculations at the SCF (self-consistent field) level, which provide a very elaborate polarization energy if adapted atomic basis sets are used, have been performed for the charged complexes studied in order to estimate the error on the polarization contribution. The relative error, 46%, is not negligible and thus, in our model, the polarization contribution has been scaled using a factor of 1.8 in the calculation as well as during the geometry optimization.

(iii) The dispersion and repulsion terms are sums of atom−atom terms. In the repulsion term, the influence of the electronic population variation on the van der Waals atomic radii in each molecular subunit is taken into account. The dispersion component includes terms up to C_{10}/R_{ij}^{10} as well as an exchange-dispersion contribution.

4.2. Basis and Multipole Distributions. The calculation of the interaction energy requires the determination of the

TABLE 1: Experimental and Calculated Permanent Dipole Moment of Phenol, Water, Methanol, and DME

	phenol	H_2O	CH_3OH	DME
this work	1.40	1.81	1.66	1.36
experimental[a]	1.45	1.85	1.70	1.30

[a] Reference 53.

multipole distribution of each molecular subunit involved in the electrostatic and polarization terms. The multipole distribution must be derived from a correlated wave function within at least a double-ζ plus polarization basis set.[42,43] Comparison between the calculated permanent moments and the experimental ones is used as a quality criterion of the calculation.

For all molecules, ab initio calculations are performed in the corresponding experimental geometry. Large Gaussian basis sets 14s7p2d/8s4p2d for oxygen and carbon and 10s2p/4s2p for hydrogen are used for water, methanol and dimethyl ether.[45] For phenol a smaller basis set, namely the 6-31G basis set of Pople [46] plus one set of polarization functions C(0.63), O(1.33), and H(0.80), is used. For systems with a small number of electrons as water and methanol, the correlated wave function is obtained by a multiconfigurational self-consistent field calculation using a homemade MCSCF program. For dimethyl ether and for phenol in its ground and ionic state, a MP2 calculation is performed with the Gaussian 94 program.[47] In this way, discrepancies not larger than 5% are obtained between calculated and experimental permanent dipole moments (Table 1). We can thus expect that the electrostatic interactions and corresponding electric fields are calculated very accurately.

4.3. Characterization of the Potential Energy Surface. The geometry of the complex is described by the six intermolecular coordinates: three coordinates of rotation (Euler angles) and three coordinates of translation (position of the mass center) of one molecule, the other being fixed.

4.3.1. Minimum Localization. The procedure used is an extension of the simulated annealing method to complicated potential energy surfaces presenting many minima and is similar to the procedure used by Liotard.[48] First of all, a random search on the surface is performed by Metropolis algorithm.[49] Second, the conformations obtained from this exploration are sorted out. Finally, the resulting conformations are optimized by a local minimization method (quasi-Newton method, BFGS [50]), and each minimum is proved by its Hessian.

4.3.2. Saddle Point Localization. The method we used is the method developed by Liotard.[51] It consists of shifting on the surface a path connecting two minima, the starting path being generated from a guessed saddle point and the two minima considered. The energetic relaxation of the path, until the highest point cannot be relaxed any further, leads to the determination of the saddle point. Such a local method, therefore, requires several starting paths in order to ensure the quality of the calculation.

5. Theoretical Results

5.1. Structure and Energetics of the Neutral 1:1 Complexes. The minimum energy configurations of the 1:1 phenol complexes with water, methanol, and DME (Figure 4) are all found to correspond to a hydrogen bond between the phenol molecule acting as a hydrogen donor and the water molecule acting as a hydrogen bond acceptor. The H bond is found to be nearly translinear, with only very small distortions relative to linearity (angle φ; Figure 5 and Table 2) and the main plane of the solvent molecule (H−O−H, H−O−C, and C−O−C, respectively) is perpendicular to the phenol plane. The well

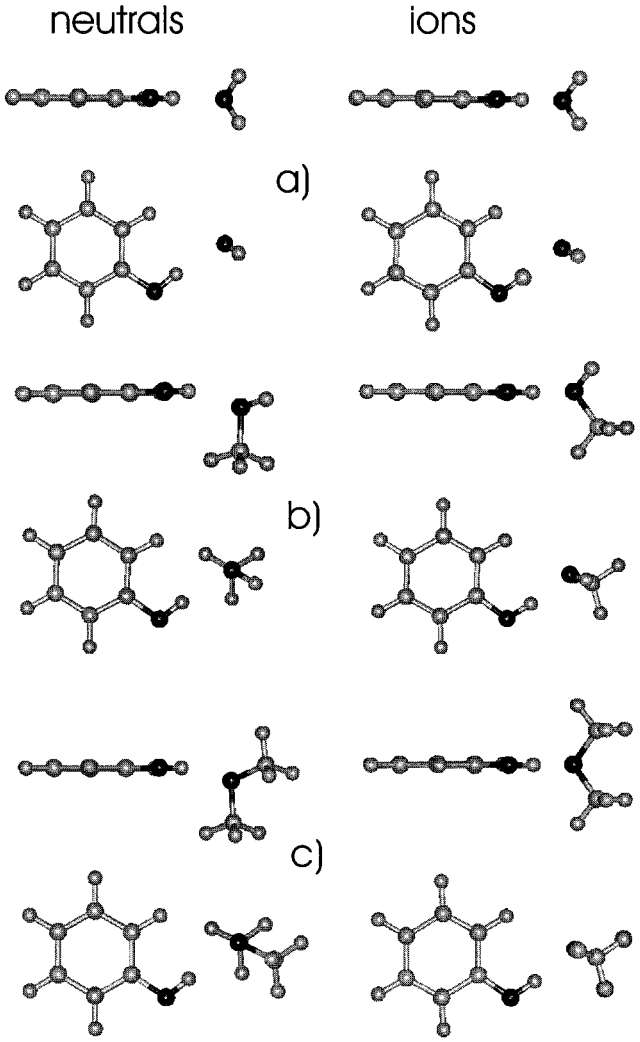

Figure 4. Calculated minimum energy structures (side and top views) of the neutral and ionic complexes found with the present semiempirical model: (a) phenol−water, (b) phenol−methanol, and (c) phenol−dimethyl ether.

depths have all been found in the same energy range (around 5.5 kcal/mol). The electrostatic forces are responsible for a large part of it and represent at least about 61% of the energy due to the attractive forces (Table 3). Configurations where phenol acts as a hydrogen bond acceptor have also been found but at higher energies (typically 2 kcal/mol higher).

Some geometrical and energetic details, however, are found to vary along the series when going from water to DME (Figure 4). In particular, whereas the minimum energy conformation of the phenol−water complex exhibits a C_s symmetry, the orientation of the solvent molecule is different with methanol or DME: the O atom is slightly shifted off the phenol plane and the O−C bond (or one of them, in the case of DME) is nearly perpendicular to the phenol plane. The decomposition of the interaction energy suggests that these distortions are due to dispersive interactions (Table 3). The dispersion interaction is indeed found to be significantly larger in the case of methanol and DME than with water although the O−O distance is larger. It represents 30% of the attractive forces for complexes with methanol and DME for only 23% with water. This corresponds to the reduced distance between the methyl group and the aromatic ring, which optimizes dispersive interactions. In other words, the H bond can be a little distorted without too much energy loss compared to the dispersive interaction gained from the distortion.

TABLE 2: Experimental and Calculated (ab Initio HF/6-31G and Semiempirical) Geometrical Parameters of the Equilibrium Conformations of the Neutral Complexes of Phenol with Water, Methanol, and DME**

		phenol−H_2O	phenol−CH_3OH	phenol−DME
φ (deg)	semiempirical	5	10	8
	ab initio	3[a]	3.5[b]	
	experimental	6.7;[c] 5[d]		
R (Å) (O−O distance)	semiempirical	2.97	3.03	3.05
	ab initio	2.90[a]	2.89[b]	
	experimental	2.93 ± 0.02;[c] 2.88[d]		
β (deg)	semiempirical	111	117	119
	ab initio	136[a]	143[b]	
	experimental	144.5;[c] 139[d]		

[a] Reference 11. [b] Reference 25. [c] Reference 18. [d] Reference 19.

TABLE 3: Components of the Interaction Energy (kcal/mol) of the Calculated Minimum Energy Structures of the 1:1 Complexes of Phenol with Water, Methanol, and DME

	electrostatic	dispersion	polarization	repulsion	total
phenol−H_2O	−6.60	−2.29	−0.96	4.45	−5.40
phenol−CH_3OH	−5.81	−2.81	−0.82	4.05	−5.39
phenol−DME	−6.04	−3.00	−0.87	4.26	−5.65

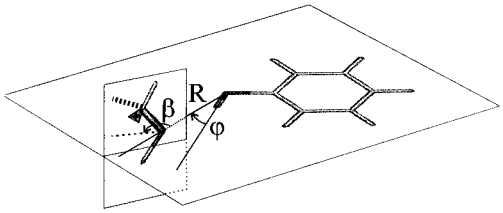

Figure 5. Structural parameters (R, φ, β) describing the translinear hydrogen bond, shown on an arbitrary conformation of the phenol−methanol water complex. The sign convention for the angle φ is such that the angle drawn in the figure is positive.

Concerning the topology of the potential energy surface, several equivalent minima are found. In the case of DME, the saddle point between the two symmetrically equivalent geometries relative to the phenol plane, which corresponds to a symmetric geometry similar to that of the complex with water, is obtained from a rocking motion of the DME molecule. However, this transition state is not found to be significant since its energy is only 0.02 kcal/mol higher than the minimum. This result suggests that the well with DME is actually very broad, in particular much larger than that with water or methanol, for which only one minimum is found for this rocking motion (symmetric with water and unsymmetric with methanol, see Figure 4). One can notice that, for each complex, the saddle point corresponding to the exchange of the substituents of the O atom in the solvent molecule is found at a much higher energy, for example at 0.85 kcal/mol relative to the minimum for phenol−water.

It is now worthwhile to note that the similar well depths (Table 3) for the three complexes disagree with the chemist's intuition, who would suggest that the electrostatic and polarization contributions and thus the well depth would increase linearly along the series, because of an increasing positive inductive effect due to the presence of methyl groups. The present calculation, in particular the values of the O-atom monopole in the multipole distribution of the solvent molecules, confirms the occurrence of such an inductive effect. However, one can notice that some other molecular features which are expected to play a role in the interaction vary in a different way: for example, the dipole moment is found to decrease along the solvent series (Table 1). The total energy actually results from a subtle compensation between several interactions, in particular electrostatic and polarization terms, which are not controlled by the charge of the O atom alone as illustrated by the energy decomposition (Table 3).

TABLE 4: Calculated Semiempirical (This Work) and ab Initio (HF/3-21G*(O)) Geometrical Parameters of the Equilibrium Conformations of the Ionic Complexes of Phenol with Water, Methanol, and DME

		phenol$^+$−H_2O	phenol$^+$−CH_3OH	phenol$^+$−DME
φ (deg)	semiempirical	−2	−3	−4
	ab initio	−6[a]		
R (Å) (O−O distance)	semiempirical	2.62	2.66	2.67
	ab initio	2.60[a]	2.52[b]	
β (deg)	semiempirical	120	124	111
	ab initio	144[a]		

[a] Reference 17. [b] Reference 16.

TABLE 5: Components of the Interaction Energy (kcal/mol) of the Calculated Minimum Energy Structures of the 1:1 Complexes of Phenol$^+$ with Water, Methanol, and Dimethyl Ether

	electrostatic	dispersion	polarization	repulsion	total
phenol$^+$−H_2O	−19.36	−4.27	−10.54	+14.33	−19.84
phenol$^+$−CH_3OH	−18.12	−4.59	−10.94	+13.38	−20.27
phenol$^+$−DME	−18.46	−5.24	−12.38	+14.58	−21.50

Like our semiempirical model, the ab initio geometry optimizations of the phenol−water complex, which have been carried out at both Hartree−Fock[11] and MP2 levels,[12] also predict a C_s complex symmetry, the O−O distances being shorter. For the phenol−methanol, only one Hartree−Fock geometry optimization has been performed,[24,25] leading to a structure similar to that of the phenol−water: the O atom is in the phenol plane and the methyl group is located far from the aromatic ring as if one hydrogen atom of water have been replaced by a methyl group. These ab initio calculations,[24,25] which do not take into account the dispersive forces for the geometry optimization, were not able to detect the symmetry breaking induced by the interaction between the methyl group and the aromatic ring.

5.2. Structure and Energetics of the Ionic 1:1 Complexes. The minimum energy configurations of these three complexes (Figure 4) are still found to correspond to a hydrogen bond, with the main plane of the solvent molecule (H−O−H, H−O−C, and C−O−C, respectively) being perpendicular to the phenol plane and with the distortion of the H bond relative to the linearity being smaller than for neutrals complexes and in the opposite sense (see the negative φ angles in Table 4; Figure 5). The main difference with neutrals is that the intermolecular O−O distance is significantly shortened, passing from 2.9 to 2.6 Å, as well as the distance between the oxygen atom of water and the hydrogen atom in the ortho ring position of phenol which goes from 2.8 to 2.5 Å. In connection with these shorter distances, because of the huge charge−dipole interaction, the energetics lies now in the 20 kcal/mol energy range (Table 5). On the other hand, practically no changes are observed in the structure along the series from water to DME: the O atom is in the phenol plane and one or two hydrogen atoms are replaced by one or two methyl groups. The dispersion energy represents now only around 14% of the energy due the attractive forces and the part of the polarization energy is strongly enhanced, passing from 9% of the attractive forces in the case of the

TABLE 6: Experimental (This Work), Semiempirical (This Work) and ab Initio Energetic Data (Well Depth D_e and Binding Energy D_0) of the Neutral and Ionic Complexes of Phenol with Water, Methanol, and DME (kcal/mol)[a]

		D_e	D_0	D_e^+	D_0^+
phenol−H_2O	semiempirical	5.40	3.66	19.84	16.73
	ab initio	6.99[b]	5.24[b]	25.90[e]	22.70[e]
	experimental		5.60 ± 0.11		18.54 ± 0.11[f]
phenol−CH_3OH	semiempirical	5.39	4.13	20.27	18.21
	ab initio	7.13[c]	5.84[c]	27.90	25.84[e]
	experimental		6.11 ± 0.18		21.40 ± 0.18[f]
phenol−DME	semiempirical	5.65	4.39[d]	21.50	19.44[d]

[a] In order to estimate the semiempirical binding energy, the ZPE contribution has been taken equal to the ZPE ab initio data. [b] Reference 11: MP2/6.31G**//HF/6-31G** level including BSSE correction; ZPE calculated at the HF/6-31G** level. [c] Reference 25: MP2/6.31G**//HF/6-31G** level including BSSE correction; ZPE calculated at the HF/6-31G** level. [d] Assuming the same ZPE as in the complex with methanol. [e] Reference 16: MP2/3.21G*(O)//HF/3-21G*(O) level including BSSE correction; ZPE estimated at the HF/3-21G*(O) level from the intermolecular frequencies of each complex and the shift of the 10 lowest intramolecular frequencies of the phenol$^+$−water complex. [f] Values obtained from the binding energies obtained in the present work and the adiabatic ionization potential precisely measured by Müller-Dethlefs and co-workers.[14−16]

neutrals to 32%. The electrostatic and polarization interactions are now so large that the energy loss due to the distortion of the H bond cannot be compensated by the gain in dispersion due to the contact between methyl group and phenol ring.

The geometries obtained for phenol$^+$−water and phenol$^+$−methanol are rather similar to the ab initio calculations performed at a modest level of theory (HF/3-21G*(O)).[16,17]

6. Discussion: Comparison between Experiment and Theory

6.1. Energetics. 6.1.1. Comparison between Experiment and Theory. The experimental data obtained in this work on the neutral species can be combined to the high-precision ionization energies of Müller-Dethlefs and co-workers[14−16,22,26,28] in order to provide experimental ionic binding energies D_0^+. These values are given in Table 6.

The comparison between experimental data, namely the binding energies D_0, and the calculated characteristics of the potential energy surface, in particular the well depths, requires the knowledge of the zero-point vibrational energy (ZPE), the intramolecular component of which are not negligible (∼30% of the total ZPE[11,26,27]). For this purpose, the ab initio ZPEs available have been combined to the well depths for both the ab initio and the present semiempirical model in order to propose theoretical D_0 values. These data, given in Table 6, are also compared with the experimental values.

For the neutral complexes, Table 6 shows that a rather good agreement is found between experiment and the ab initio values, even if these values appear to be slightly too small. On the other hand, agreement with semiempirical model is clearly not so good.

For the sake of consistency, we have only considered for phenol−water and phenol−methanol ab initio calculations at the same level of theory, MP2/6-31G**//HF/6-31G** corrected for BSSE and ZPE (HF/6-31G**). However, on expanding the basis set from double to triple-ξ,[11] the binding energy D_0 of phenol−water is decreased by 0.94 kcal/mol (D_0 = 4.30 kcal/mol), the ZPE being not really modified (1.78 kcal/mol versus 1.75 kcal/mol). The well depth (D_e) is then decreased by ≈13%, the BSSE contribution remaining an important correction which represents 30% of the well depth. The difference between the two ab initio values of D_0 for the phenol−water complex (5.24 and 4.30 kcal/mol) gives an order of magnitude of the error in such calculations that may be as large as about 1 kcal/mol. This suggests that the ab initio value did not converge, either with the basis set and maybe or with the level of theory. In our semiempirical model, values of D_e are systematically 1.5 kcal/mol lower than the experimental ones, which suggests that some van der Waals parameters might be reconsidered. This is also consistent with the slightly too large O−O distances found in the semiempirical model compared to the experimental or ab initio data (Table 2). Furthermore, in the semiempirical calculations, only the intermolecular degrees of freedom are optimized while the ab initio calculations have been carried out relaxing both intra- and intermolecular degrees of freedom.

However, the present semiempirical model and the ab initio calculations predict correctly the D_0 change when going from water to methanol, if one compares with experiment. The values found for the well depths of phenol−water and phenol−methanol are very close to one another. Consequently, it turns out that the vibration zero-point energy is mainly responsible for the difference in the binding energies D_0, in contrast to the interpretation, in terms of an eventual positive inductive effect, due to the methyl groups sometimes invoked.[16,27]

For the ionic complexes, Table 6 suggests that the semiempirical values, slightly too small, are better than the ab initio ones, which are found to significantly overestimate the binding energies. Indeed, the ab initio calculations were carried out with a modest 3-21G*(O) basis set, which is known to give too large well depths and very important BSSE contributions.

6.1.2. Comparison with Experimental Data on Other Similar Complexes. In order to test the internal consistency of the experimental data, it seems worthwhile to compare these results to those obtained very recently in Leutwyler's group on a very similar system: the complexes of 1-naphthol with water, methanol, and ammonia.[31] The D_0 found for the 1-naphthol−water complex (5.82 ± 0.20 kcal/mol) is close to that obtained in the present work, in fair agreement with the fact that 1-naphthol and phenol have similar acidities in solution. However, a noticeable disagreement is found between the complexes with methanol. Surprisingly, the value reported by Leutwyler (7.56 ± 0.40 kcal/mol)[31] is much higher than the present value on phenol−methanol and very close to that obtained, in the same work, with ammonia (7.663 ± 0.015 kcal/mol).[31] Such an observation, a priori unexpected owing to the large difference in the gas-phase proton affinities of methanol and ammonia, suggests that the measurement on 1-naphthol−methanol can be affected by an experimental artifact. This feeling is supported by the ab initio calculations performed on the complexes of phenol[11] and 1-naphthol.[31] Small variations in calculated binding energies are indeed found when going from water to methanol with phenol (0.55 kcal/mol [11,27]) and 1-naphthol (0.60 kcal/mol [31]). This trend is moreover confirmed by the present experimental difference between phenol−water and phenol−methanol (0.51 kcal/mol).

The present work allows us also to discuss the surprising experimental results of Mikami and co-workers on the phenol−ammonia complex.[23] Using a methodology similar to that of the present work, these authors report a binding energy of 5.15 kcal/mol for this complex, which seems to be small compared to that found for the phenol water complex (5.60 kcal/mol in the present work) and for the 1-naphthol−ammonia complex (7.663 kcal/mol [31]). In addition, anomalously high fragmentation ratios are reported (40%) for a complex which is expected to be more bound than phenol−water. These data can be accounted for assuming that laser intensity is high enough to cause the absorption of a third photon in the ionic complex. In such a case, fragmentation takes place in the excited state of the ion, leading to the breaking of the weakest bond, i.e., the phenol$^+$−ammonia bond. Thus the fragmentation spectra recorded reflect more the ability to excite the complex ion rather than the appearance potential of the phenol$^+$ fragment in the ground-state ion. Finally, no reliable D_0 value can be derived from such an experiment.

6.1.3. Comparison between Two Experimental H-Bond Indicators: D_0 and $\delta\nu_{OH}$. The present experimental binding energy D_0 obtained in this work allows us to test the pertinence of the spectral red shift $\delta\nu_{OH}$ of the OH vibration in the complex as an experimental indicator of the strength of H bond. Infrared measurements of the OH vibration frequency of phenol in gas phase size-selected complexes have indeed been reported recently by Mikami and co-workers.[13,29] A significant difference (∼30%) is found in $\delta\nu_{OH}$ between the phenol−water and phenol−methanol complexes (133 and 201 cm^{-1}, respectively). The comparison with the present binding energies shows that the spectral shift reflects neither the same well depths D_e of these complexes nor their very similar binding energies D_0, which differ by only ∼9%. This suggests that the spectral shift $\delta\nu_{OH}$ cannot be considered as a precise indicator, capable of distinguishing properly between complexes that are so similar, even if one can guess that it should give satisfactory approximate results when comparing complexes with bases having very different proton affinities.

6.2. Geometry: Interpretation of the Threshold Photoelectron Spectra of the Phenol Complexes. The present semiempirical calculations have highlighted the role of the dispersive interactions in the geometry of the neutral complexes. The possibility of calculating the ion structure at the same level of theory allows us to characterize the final state of the ionic complex following ionization. In particular, it has been possible to calculate the excess energy deposited in the ion by the ionization process. For this purpose, it has been assumed that (i) the ionization is a vertical process between the S_1 neutral state and the ion, according to the Franck−Condon principle applied to the intermolecular vibrations of the complex, (ii) the excess energy can be obtained by the energy difference between the ionic state reached by the vertical transition (i.e., the ion complex having the S_1 state geometry) and the ionic equilibrium configuration, and (iii) the geometry of the S_1 state has been considered as identical to that of the ground S_0 state, this assumption being justified by the small electronic shift (350 cm^{-1})[11] compared to the S_0 binding energy (1960 cm^{-1}) as well as by the similar dipole moments of the phenol molecule in these two electronic states.[52] For the three complexes of phenol with water, methanol, and DME excess energies have all been found in the 4 kcal/mol energy range (4.05, 4.64, and 4.57 respectively). These values can be considered useful in interpreting the threshold photoelectron (ZEKE) spectra of the phenol complexes by Müller-Dethlefs and co-workers.[14−16,22,26,28]

All ZEKE spectra of the phenol complexes, which illustrate the density of intermolecular states accessible in the ion by a photoionization process near the threshold, exhibit a broad Franck−Condon envelope. That is, in all spectra, whatever the solvent molecule, a progression showing at least two overtones is seen for the H-bond stretching mode.[14−16,22,26,28] For the complex with water, however, this progression is single. In the case of methanol and DME, several other intermolecular modes are active and the density of intermolecular levels reachable is much larger. Up to now, this property was not accounted for on the basis of ab initio calculations alone, which indicated a similar geometry for both neutral and ionic states of the complexes. The present semiempirical results allow us to account for the line density in the ZEKE spectra on the basis of the geometries of Figure 4. For the water complex, the major change between neutral and ion consists in a shortening of the H bond, without any symmetry change, which accounts for the excitation of the H-bond stretching mode alone. The excess energy calculated, ∼4 kcal/mol, corresponds to the excitation of 5 quanta of the H-bond stretching mode, in qualitative agreement with the observation. The similar geometries for the ground and ionic state suggest that no other mode will be active, again in agreement with the observation. In the case of complexes with methanol or DME, however, in addition to the excitation of the stretching mode, the intermolecular modes corresponding to the geometry change between the equilibrium conformations of the neutral and ionic species are also expected to be active, which qualitatively explains the density of lines in the ZEKE spectra of these species. The calculated excess energy differences between these two complexes and that with water suggest that the corresponding energy deposited in these modes is relatively small, but owing to their small frequencies (typically 40 cm^{-1}), this amount of energy can correspond to progressions having more than four overtones.

7. Conclusion

The present paper provides both experimental and theoretical benchmarks for the binding energy of a typical H bond in the gas phase, namely complexes of phenol with water and methanol. For the first time, reliable experimental energetics data are proposed and can be considered, with some recent measurements by Leutwyler and co-workers[31] on the complexes of 1-naphthol, as a first data set for the experimental approach to the energetics of gas-phase hydrogen bonds involving an aromatic proton donor molecule.

Besides experiment, molecular modeling using a semiempirical model has allowed us to get some insight in the role of the several interactions involved in the hydrogen bond. Thus, a careful analysis suggests that, even in an apparently coherent series of solvent molecules like water, methanol, and dimethyl ether, a simple picture like the positive inductive effect expected by the chemist's intuition does not allow the description of the energetic trends within the solvent series. In particular, the semiempirical calculations emphasize the role of the dispersive interactions in the geometry of these species, especially in the case of the existence of an alkyl group in the solvent molecule. Such effects are difficult to account for with the ab initio techniques, in which the geometry optimization is generally not carried out at a level which takes into account the dispersion contribution. Ab initio techniques are nevertheless necessary in order to provide the change in the intramolecular vibrations upon hydrogen-bond formation. The relevance of this semiempirical model is also demonstrated for the determination of the ionic state geometry as well as for the characterization of the

ionization process, in particular, the estimation of the energy deposited upon ionization.

References and Notes

(1) Pimentel, G. C.; McClellan, A. L. *The Hydrogen Bond*; Freeman: San Francisco, 1960.
(2) Zwier, T. S. *Annu. Rev. Phys. Chem.* **1996**, *47*, 205.
(3) Abe, H.; Mikami, N., Ito, M. *J. Phys. Chem.* **1982**, *86*, 1768.
(4) Fuke, K.; Kaya, K. *Chem. Phys. Lett.* **1983,** *94*, 97.
(5) Gonohe, N.; Abe, H.; Mikami, N.; Ito, M. *J. Phys. Chem.* **1985**, *89*, 3642.
(6) Lipert, R. J.; Colson, S. D. *J. Chem. Phys.* **1988**, *89*, 4579.
(7) Lipert, R. J.; Colson, S. D. *J.. Phys. Chem.* **1989**, *93*, 135.
(8) Lipert, R. J.; Colson, S. D. *J. Phys. Chem.* **1988**, *92*, 3801.
(9) Stanley R. J.; Castleman, A. W., Jr. *J. Chem. Phys.* **1991**, *94*, 7744.
(10) Hartland, G. V.; Henson, B. F.; Venturo, V. A.; Felker, P. M. *J. Phys. Chem.* **1992**, *96*, 1164.
(11) Schutz, M.; Burgi, T.; Leutwyler, S. *J. Chem. Phys.* **1993**, *98*, 3763.
(12) Feller, D.; Feyereisen, M. W. *J. Comput. Chem.* **1993**, *14*, 1027.
(13) Tanabe, S.; Ebata, T.; Fujii, M.; Mikami, N. *Chem. Phys. Lett.* **1993**, *215*, 347.
(14) Dopfer, O.; Reiser, G.; Müller-Dethlefs, K.; Schlag, E. W.; Colson, S. D. *J. Chem. Phys.* **1994**, *101*, 974.
(15) Müller-Dethlefs, K.; Dopfer, O,; Wright, T. G. *Chem. Rev.* **1994**, *94*, 1847 and references therein.
(16) Dopfer, O. Thesis, Technische Universität München, 1994.
(17) Hobza, P.; Burcl, R.; Spirko, V.; Dopfer, O.; Müller-Dethlefs, K.; Schlag, E. W. *J. Chem. Phys.* **1994**, *101*, 990.
(18) Berden, G.; Meerts, W. L.; Schmitt, M.; Kleinermans, K. *J. Chem. Phys.* **1996**, *104*, 972.
(19) Gerhards, M.; Schmitt, M.; Kleinermanns, K.; Stahl, K. *J. Chem. Phys.* **1996**, *104*, 967.
(20) Ebata, T.; Mizuochi, N.; Watanabe, T.; Mikami, N. *J. Phys. Chem.* **1996**, *100*, 546.
(21) Watanabe, H.; Iwoata, S. *J. Chem. Phys*. **1996**, *105*, 420.
(22) Dopfer, O., Melk, M.; Müller-Dethlefs, K. *Chem. Phys. Lett.* **1996**, *207*, 437.
(23) Mikami, N.; Okabe, A.; Suzuki, I. *J. Phys. Chem.* **1988**, *92*, 1858.
(24) Gerhards, M.; Beckmann, K.; Kleinermanns, K. *Z. Phys. D* **1994**, *29*, 223.
(25) Schiefke, A.; Deusen, C.; Jacoby, C.; Gerhards, M.; Schmitt, M.; Kleinermanns, K.; Hering, P. *J. Chem. Phys.* **1995**, *102*, 9197.
(26) Wright, T.; Cordes, E.; Dopfer, O.; Müller-Dethlefs, K. *J. Chem. Soc., Faraday. Trans.* **1993**, *89*, 1609.
(27) Schmitt, M.; Muller, H.; Henrichs, U.; Gerhards, M.; Deusen, C.; Kleinermanns, K. *J. Chem. Phys.* **1995**, *103*, 585.
(28) Dopfer, O.; Wright, T. G.; Cordes, E.; Müller-Dethlefs, K. *J. Am. Chem. Soc.* **1994**, *116*, 5880.
(29) Iwasaki, A.; Fujii, A.; Watanabe, T.; Ebata, T.; Mikami, N. *J. Phys. Chem.* **1996**, *100*, 16053.
(30) Knochenmuss, R.; Cheshnovsky, O.; Leutwyler, S. *Chem. Phys. Lett.* **1988**, *144*, 317.
(31) Burgi, T.; Droz, T.; Leutwyler, S. *Chem. Phys. Lett.* **1995**, *246*, 291.
(32) Le Barbu, K.; Brenner, V.; Millié, Ph.; Lahmani, F.; Zehnacker-Rentien, A. *J. Phys. Chem. A*, in press.
(33) Guillaume, C.; Le Calvé, J.; Dimicoli, I.; Mons, M. *Z. Phys. D* **1994**, *32*, 157.
(34) Anderson, S. L.; Gordman, L.; Krogh-Jepersen, K.; Ozkabak, A. G.; Zare, R. N.; Zheng, C. *J. Chem. Phys.* **1985**, *82*, 5329.
(35) Krause, H.; Neusser, H. J. *J. Chem. Phys.* **1993**, *99*, 6278.
(36) Ernstberger, B.; Krause, H.; Kiermeier, A.; Neusser, H. J. *J. Chem. Phys.* **1990**, *92*, 5285.
(37) Claverie, P. *Intermolecular Interactions: from diatomics to biopolymers*; Wiley: New York, 1978; Chapter 2.
(38) Langlet, J.; Claverie, P.; Boeuvre, F. J. C. *Int. J. Quantum Chem.* **1981**, *19*, 299.
(39) Hess, O.; Caffarel, M.; Caillet, J.; Huiszoon, C.; Claverie, P. In *Proceedings of the 44th international meeting on modeling of molecular structures and properties*; Rivail, J. L., Ed.; Elsevier: Amsterdam, 1990; p 323.
(40) Brenner, V.; Martrenchard-Barra, S.; Millié, Ph.; Dedonder-Lardeux, C.; Jouvet, C.; Solgadi, D. *J. Phys. Chem.* **1995**, *99*, 5848.
(41) Desfrançois, C.; Abdoul-Carime, H.; Khelifa, N.; Schermann, J. P.; Brenner, V.; Millié, Ph. *J. Chem. Phys.* **1995**, *102*, 4952.
(42) Brenner, V.; Millié, Ph. *Z. Phys. D.* **1994**, *30*, 327.
(43) Millié, Ph.; Brenner, V. *J. Chim. Phys. (Paris)* **1995**, *92*, 428.
(44) Vigné-Maeder, F.; Claverie, P. *J. Chem. Phys.* **1988**, *88*, 4934.
(45) van Duijneveldt, F. B. *IBM Res. Rep.* **1971**, *RJ945*.
(46) Hehre, W. J.; Radom, C.; Schleyer, P. v. R.; Pople, J. A. *Ab Initio Molecular Orbital Theory*; Wiley Interscience: New York, 1986.
(47) Frisch, M. J.; Trucks, G. W.; Schlegel, H. B.; Gill, P. M. W.; Johnson, B. G.; Robb, M. A.; Cheeseman, J. R.; Keith, T.; Petersson, G. A.; Montgomery, J. A.; Raghavachari, K.; Al-Laham, M. A.; Zakrzewski, V. G.; Ortiz, J. V.; Foresman, J. B.; Cioslowski, J.; Stefanov, B. B.; Nanayakkara, A.; Challacombe, M.; Peng, C. Y.; Ayala, P. Y.; Chen, W.; Wong, M. W.; Andres, J. L.; Replogle, E. S.; Gomperts, R.; Martin, R. L.; Fox, D. J.; Binkley, J. S.; Defrees, D. J.; Baker, J.; Stewart, J. P.; Head-Gordon, M.; Gonzalez, C.; Pople, J. A. *Gaussian 94, Revision C.2*; Gaussian, Inc.: Pittsburgh, PA, 1995.
(48) Bockish, F.; Liotard, D.; Rayez, J. C.; Duguay, B. *Int. J. Quantum Chem.* **1992**, *44*, 619.
(49) Metropolis, N.; Rosenbluth, A.; Rosenbluth, M.; Teller A.; Teller, E. *J. Chem. Phys.* **1953**, *21*, 1087.
(50) Flether, R. *Comput. J.* **1970**, *13*, 317. Goldfarb, D. *Math. Comput*. **1970**, *24*, 23. Shanno, D. F. *Math. Comput.* **1970**, *24*, 647.
(51) Liotard, D. *Int. J. Quantum Chem.* **1992**, *44*, 723.
(52) Lorentzon, J.; Malmqvist, P.-A.; Fülscher, M.; Roos, B. O. *Theor. Chim. Acta* **1995** *91*, 91.
(53) *CRC Handbook of Chemistry and Physics*, 62nd ed.; CRC Press: Boca Raton, FL, 1981; p E60−62.